Graphite versus graphene: plasmonic nanopore DNA sequencing

Bashir Fotouhi*

Faculty of Electrical and Computer Engineering, University of Kurdistan, Kurdistan, Iran

(Received 29 April 2022; Revised 12 February 2023)

The plasmonic-based graphite- and graphene-nanopores have been investigated by employing the hybrid quantum/classical scheme (HQCS). Transverse, longitudinal, and total absorption spectra obtained from HQCS are analyzed for the graphite and graphene nanopores. Analyses were examined for each structure in the presence of deoxyribonucleic acid (DNA) nucleobases. The simple excitation of the total mode in graphene nanopore shows the best selectivity for DNA sequencing. A novel method based on the transverse and longitudinal modes in a time-series approach has been proposed for selectivity improvements. In the proposed time-series method, the outstanding results show that graphite nanopore is more sensitive than and as selective as graphene nanopore. This paper suggests that time-step analysis of the plasmonic absorption in the graphite nanopore is a promising method for DNA sequencing.

Document code: A **Article ID:** 1673-1905(2023)06-0353-6

DOI https://doi.org/10.1007/s11801-023-2071-8

Plasmonic waves have been investigated for deoxyribonucleic acid (DNA) sequencing[1], single-molecule detection[2], particle sorting[3], and object trapping[4]. Surface plasmon resonance (SPR) mechanisms are susceptible to the structure shape and size[1,3]. One of the significant aspects of interest for SPR is single-molecule sensing developed in the last few years[1,2]. Nanopore-based DNA sequencing has been a growing field of research in the last two decades[5-7]. Ionic and tunneling currents, Raman spectroscopy, and plasmonic resonances are used in these studies[5-7]. Two-dimensional materials, such as graphene and MoS_2, are in great interest due to their biocompatibility, comparable thicknesses to the DNA nucleobase, and robust mechanical properties[5-8]. Indeed, plasmonic signals were used in these materials to sequence DNA molecules[8,9]. Most recent studies prove that pure classical calculations of SPR in graphene nanopores and metal bowtie nanostructures show a superior sensitivity to the DNA nucleotides[10]. As also proved in classical molecular dynamics calculations, the interband plasmons in graphene can control the translocation speed of the DNA molecule through graphene nanopore[11]. The practical challenges for graphite nanopores are less than graphene ones. However, graphite nanopores are less studied for DNA sequencing. The ionic current in nanocrystalline graphite was proposed for DNA translocation sense[12].

To study the viability of SPR in graphite or graphene for single-molecule sensing, pure classical methods[13] are less valid in this scale, and pure quantum-mechanical methods are not efficient[9,10]. The hybrid quantum/classical scheme (HQCS) has been developed based on the combinations of time-domain density functional theory (TDDFT) and classical Maxwell equations[14-16]. This hybrid scheme was used to predict molecule sensing via plasmon coupling in silver and gold nanoparticles[15,17-20]. HQCS is accurate in the molecular scales compared to pure classical methods such as discrete dipole approximation[13,15,19]. After fitting graphite and graphene permittivities, their absorption properties at the presence of DNA nucleobases are studied, and a new time-series method is proposed for sequencing DNA molecules.

The HQCS divides proposed structure into quantum and classical subsystems. The quantum subsystem is treated using TDDFT, and the classical one is treated by the finite difference time domain (FDTD) method. These subsystems are illuminated separately, but also affected by other electrostatic potentials[15,21]. This study considers the DNA molecule as the quantum subsystem and the graphene or graphite sheet as the classical one. For the classical subsystem in the HQCS, the permittivity is modeled as a linear combination of Lorentz oscillators described as

$$\varepsilon(\omega)=\varepsilon_{\mathrm{Re}}(\omega)+\mathrm{i}\varepsilon_{\mathrm{Im}}(\omega)=\varepsilon_{\infty}+\varepsilon_0\sum_j\frac{\beta_j}{\omega_j^2-\mathrm{i}\omega\alpha_j-\omega^2},\quad(1)$$

where β_j, ω_j and α_j are parameters to fit the desired model to the experimental permittivities. As desired in the current implementation of HQCS[15], we assume $\varepsilon_\infty=\varepsilon_0$ and ω is the frequency in electron-volt. Also, ε_R and ε_I are the real and imaginary parts of the permittivity, respectively. The best fitted permittivities are achieved by the method described in Ref.[15]. The experimental permittivities for graphite and graphene are reported in Refs.[21—24]. The fitting frequency ranges from 2 eV to

*E-mail: b.fotouhi@uok.ac.ir

8 eV for graphite and graphene. Tab.1 shows all the Lorentz parameters to fit the graphite and graphene permittivities. Fig.1 shows experimental and fitted data for the real and imaginary parts of the permittivity for graphite and graphene. For the HQCS calculations, the GPAW codes were used[25,26].

Tab.1 Lorentzian parameters β_j (eV^2), ω_j (eV) and α_j (eV) for permittivities of graphite and graphene

	Graphite	Graphene		Graphite	Graphene
β_0	68.190	−16.931	β_4	−8.348	79.312
ω_0	4.473	1.042	ω_4	1.758	11.999
α_0	1.639	0.437	α_4	1.421	0.693
β_1	76.260	17.681	β_5	31.795	23.460
ω_1	1.758	5.638	ω_5	0.611	2.089
α_1	2.822	2.999	α_5	0.100	2.777
β_2	−32.157	35.385	β_6	16.947	27.177
ω_2	0.100	4.510	ω_6	11.999	0.995
α_2	0.100	1.151	α_6	5.690	0.518
β_3	−19.633	13.929	β_7	199.999	42.412
ω_3	1.291	7.564	ω_7	12.000	3.721
α_3	3.366	2.999	α_7	0.100	2.999

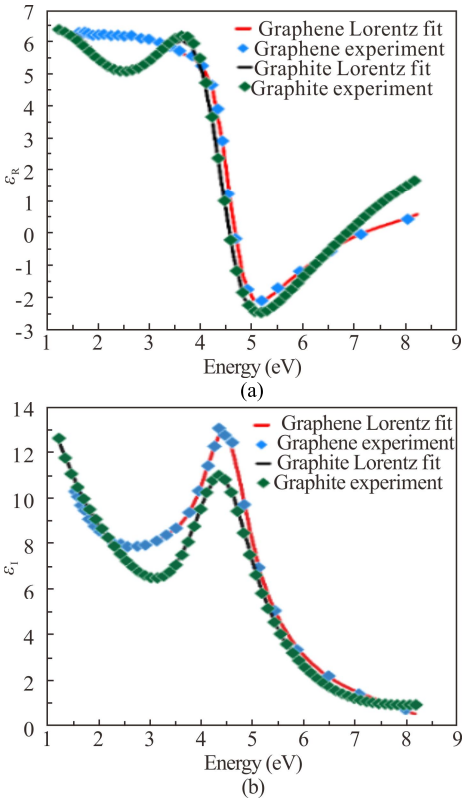

Fig.1 Comparison of experimental and Lorentzian representation of (a) real and (b) imaginary parts of permittivities for graphite and graphene

Fig.2 demonstrates the graphene and graphite sheets with a nanopore at the center of the sheet. Each structure can be illuminated by transverse, longitudinal, and total incident lights. The total mode uses both transverse and longitudinal excitations. The source energy ranges from 2 eV to 8 eV, where interband plasmons strongly influence the absorption spectra[9,10]. The interband plasmons in graphene and graphite are highly affected by the small-size effects[9,10,27,28]. Both the graphite and graphene lengths are 3 nm. The pore diameter is about 2 nm. In Fig.3, absorption spectra for graphite and grapheme nanopore obtained from the HQCS method are shown. HQCS results are predictable and similar to the classical calculations[15,18], while no quantum subsystem presents. For the graphene nanopore, one dominant mode is mainly related to the interband plasmon of graphene. The peak frequency is 4.75 eV (260 nm wavelength). HQCS results for graphene nanopores are in excellent agreement with the previous studies done by the abinitio calculations and discrete dipole approximation methods[10,13]. These results also agree with those experimentally obtained by ZHOU et al[27] and DESPOJA et al[28].

Fig.3 shows the transverse, longitudinal, and total modes of the absorption spectra for graphene and graphite nanopores, respectively. It can be seen that the amount of absorption in the transverse modes is always more considerable than longitudinal modes. However, in the graphite, and because the sheet thickness tends to be comparable to the graphite length, the amount of absorption in the longitudinal mode is more comparable to that of the transverse mode. In the total modes, the graphene and graphite nanopores have one resonance frequency at 4.75 eV and 5.1 eV, respectively. This resonance frequency in the photoabsorption spectrum are mainly related to the valance electron's collective excitation, interband plasmons[9,10]. In the graphite, the absorption spectrum peak is broader than the graphene. One possible reason is that the inter-layer bonds in the graphite introduce new transition energies. The graphene nanopore does not show any resonance peak in the longitudinal mode. The graphene thickness is minimal, and no collective excitation is produced.

As depicted in Fig.4, the transverse, longitudinal, and total modes of the absorption spectra are highly affected by DNA nucleobases. At the presence of each DNA nucleobases, the total, transverse, and longitudinal modes of the absorption spectra for graphene and graphite nanopores are shown in Fig.4. Presenting each DNA nucleobase to thenanopore results in new peaks or creates a remarkable shift in the peak resonance frequency.

As shown in Fig.4, two main resonance frequencies in the absorption spectrum exist, ω_{R1} and ω_{R2}. In total mode and G nucleobase, the first resonance frequency, ω_{R1}, was shifted to higher energy. The second resonance frequency, ω_{R2}, was introduced to the absorption spectrum for other nucleobases. None of the DNA nucleobases could create the second resonance frequency in graphite's total and longitudinal absorption spectra (see Fig.4). However, the energy of the resonance peak is slightly shifted to ~5.35 eV due to presenting DNA nucleobases.

Two parameters are defined to compare the applicability of graphite and graphene nanopores for DNA sequencing[9,10]. First, the sensitivity shows how the proposed method is sensitive to any DNA nucleobases regardless of the type of the nucleobase.

Second, the selectivity shows how the proposed method is selective between all DNA nucleobases. The sensitivity factor is defined as the average absolute relative shift of the absorption peaks due to the presence of all DNA nucleobases. The selectivity between two nucleobases is defined as the sum of the absolute relative shift of the absorption peaks, relating to the change of DNA nucleobase type. For example, if a process has high selectivity between A and T but low selectivity between T and G nucleobases, it is not proper for DNA sequencing. That is why the minimum amount of the selectivity factor is assigned to the final selectivity of the proposed method. Exact definition for the sensitivity and selectivity factors can be found in Refs.[6—10].

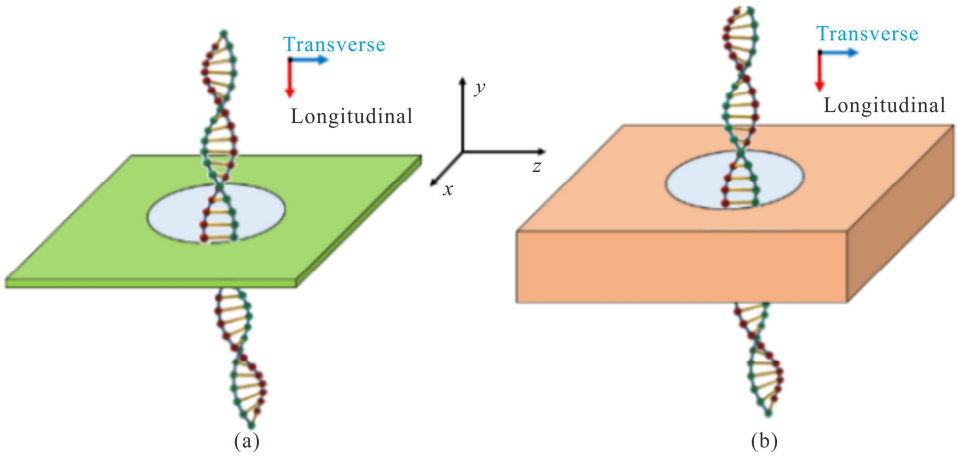

Fig.2 Schematic illustration of (a) graphene and (b) graphite nanopores with a DNA molecule passing the pore (The transverse and longitudinal modes are used to illuminate the proposed structures)

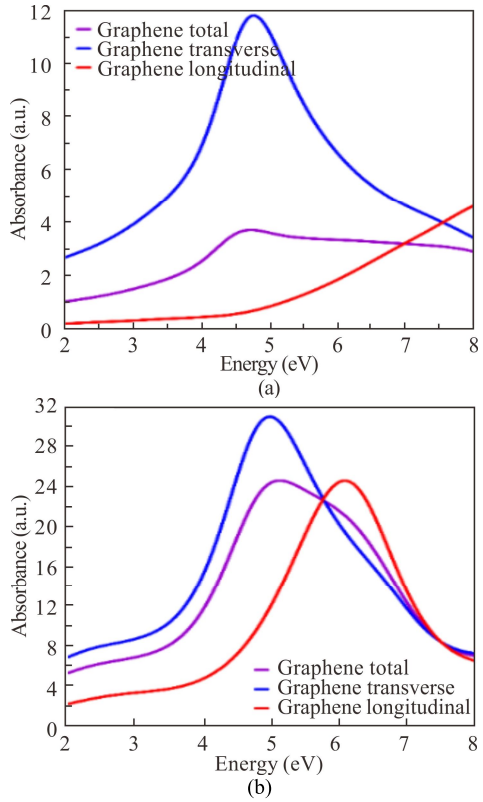

Fig.3 Absorption spectra for (a) graphene and (b) graphite (Both the graphite and graphene lengths are 3 nm; The pore diameter is about 2 nm)

Fig.5 shows the sensitivity and selectivity factors for each transverse, longitudinal, and total mode of the graphite and graphene nanopores. Fig.5(a) and (b) show the selectivity factor between all DNA nucleobases presented to the graphene and graphite nanopores, respectively. In Fig.5(c), the sensitivity to presenting DNA nucleobases for the graphite and graphene nanopores is shown. The sensitivity and selectivity factors are described for each transverse, longitudinal, and total mode. In Fig.5, if any selectivity factor equals one, it means that the proposed method is utterly selective between these two DNA nucleobases. For example, in Fig.5(a), the selectivity factor between A and G nucleobases is one, meaning that the G and A nucleobases can be easily distinguished by the longitudinal excitation of the graphene nanopore. In the cases where the selectivity is closed to 0.001, the two nucleobases cannot be distinguished. For example, in Fig.5(a), the longitudinal mode of the graphene nanopore cannot distinguish the A and C nucleobases. Final selectivity factor for each structure is theminimum selectivity between all pairs. As shown in Fig.5, the selectivity factors for the transverse, longitudinal, and total modes in the graphene nanopore are 0.017 8, 0, and 0.039 8, respectively. The minimum selectivity factor for all the graphite-based modes is 0.

As shown in Fig.5(c), the sensitivity factor for the longitudinal mode of the graphite is higher than that for all the modes in graphene. In the transverse mode, the graphite sensitivity is higher than graphene. However, in the total mode, the graphene sensitivity is higher than that of graphite. Although the simple excitation of the graphite nanopore is the best sensitive case for DNA translocation sense, it cannot be used for DNA sequencing. Thus, a new time-series method is intoruduced to improve selectivity of the graphite for plasmonic DNA sequencing.

Fig.6 demonstrates absorption spectrum analysis in a

time-series manner. The source light is illuminated through an objective section, and plasmon-enhanced absorption occurs in the nanopore. Three detectors are used to measure the light source's intensities and reflected and transmitted lights. The absorption spectrum is constructed by adding the detector's signals. The light source and objective parts can be tuned to illuminate the

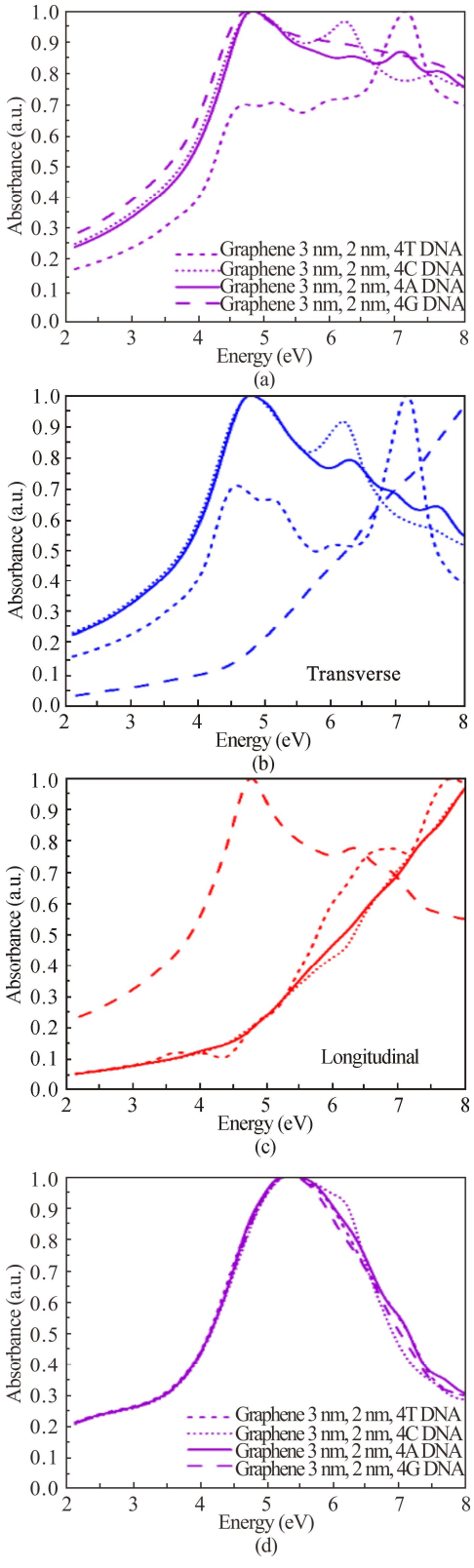

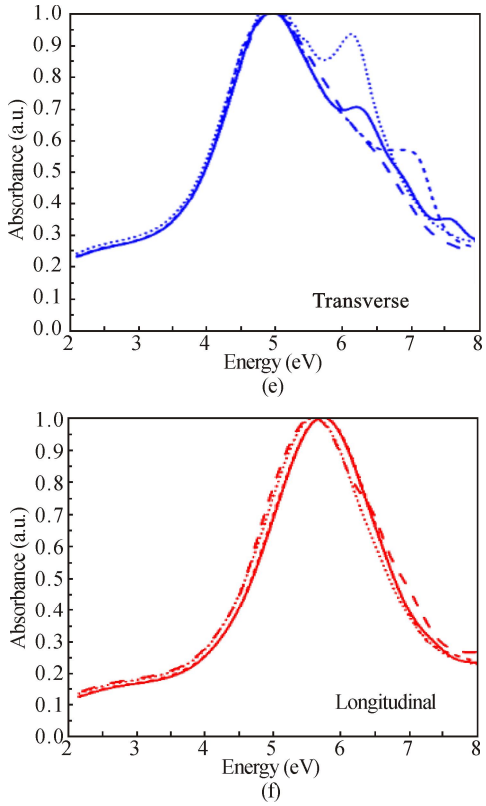

Fig.4 Effect of presenting DNA nucleobases into the graphite and graphene nanopores on the normalized photoabsorption, transverse and longitudinal modes for (a)—(c) grapheme and (d)—(f) graphite

nanopore at the transverse or longitudinal modes. Every two successive spectra in the time-series signals are analyzed to determine the type of the DNA nucleobase. Fig.7 shows selectivity between all DNA nucleobases for the graphite and graphene nanopores in the time-series approach. The graphene nanopore selectivity between the G and T nucleobases is enormously improved. For both simple excitation and time-series manners, the minimum selectivity for graphene nanopore is 0.017 8. In the time-series approach, compared to the simple excitation method of graphite, the minimum selectivity was increased from 0 to 0.01. The results for the graphite are comparable to the graphene nanopore reported in Ref.[9].

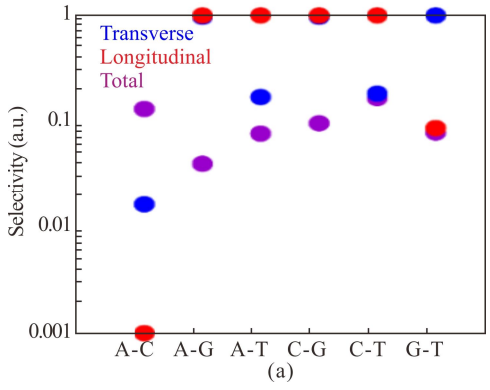

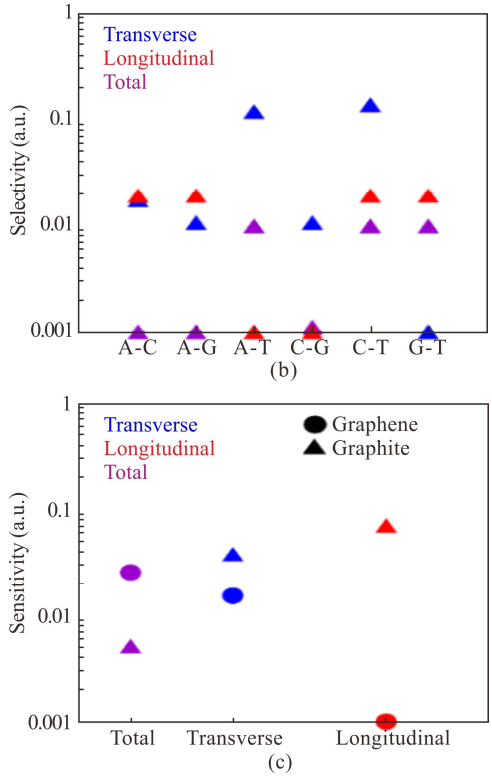

Fig.5 (a) (b) The selectivity and (c) sensitivity for graphene and graphite in the transverse, longitudinal, and total modes

Plasmon-enhanced optical absorption in graphite nanopores has higher sensitivity compared to graphene. Our sensitivity factors for graphene nanopores are comparable to those obtained by the electron energy loss spectrum[9]. From the practical perspective, using the absorption spectrum is more feasible than the electron energy loss spectrum[9,10]. Graphite has advantages over the graphene nanopore for practical DNA sequencing, more effective DNA translocation speed reduction that is related to the higher electric field enhancements in graphite which are much more substantial than graphene[29].

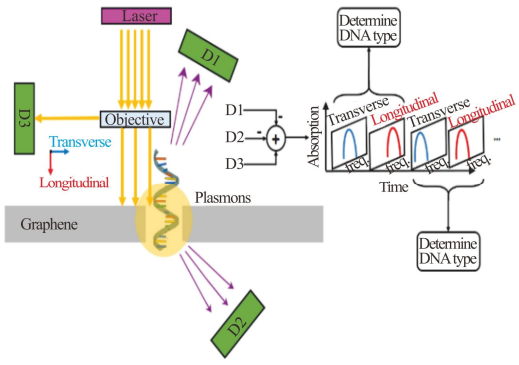

Fig.6 In graphite nanopore, two successive absorption spectra in the time-series signals analyzed to determine the type of the DNA nucleobase

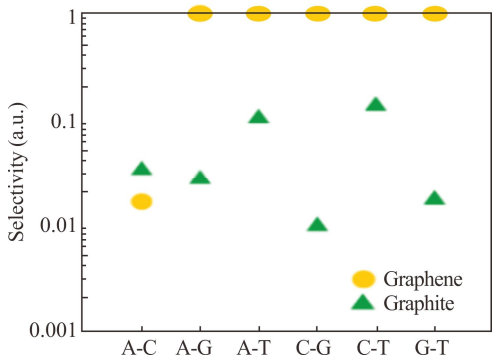

Fig.7 Selectivity factors between all DNA nucleobases for the graphite and graphene nanopores in the time-series approach

In summary, the HQCS was used to analyze transverse, longitudinal, and total modes of the absorption spectra for graphite and graphene nanopores in the presence of DNA nucleobases. The results indicate that graphite shows higher sensitivity to the DNA nucleobases compared to graphene. According to the low selectivity, simple excitation of graphite nanopore cannot be used for DNA sequencing. Otherwise, the graphene nanopores are selective enough to sequence DNA molecules. A time-series approach has been investigated to improve the graphite nanopore selectivity for DNA sequencing. The proposed time-series analysis shows higher sensitivity and selectivity than other plasmonic-based structures. This paper suggests that time-step analysis of the plasmonic absorption in the graphite nanopore is a promising method for DNA sequencing.

Ethics declarations

Conflicts of interest

The authors declare no conflict of interest.

References

[1] QIU H, ZHOU W, GUO W. Nanopores in graphene and other 2D materials：a decade's journey toward sequencing[J]. ACS nano, 2021, 15(12)：18848-18864.

[2] MOHAMMADI M M, BAVI O. DNA sequencing：an overview of solid-state and biological nanopore-based methods[J]. Biophysical reviews, 2021, 14：99-110.

[3] FARAMARZI V, AHMADI V, HEIDARI M, et al. Interband plasmon-enhanced optical absorption of DNA nucleobases through the graphene nanopore[J]. Optics letters, 2022, 47(1)：194-197.

[4] WU J X, WANG Q, SONG B B, et al. Fiber-coupler-based microfluidic system for trapping of DNA biomolecules[J]. Optoelectronics letters, 2019, 15(6)：476-480.

[5] FOTOUHI B, FARAMARZI V, AHMADI V. DNA sequencing by Förster resonant energy transfer[J]. Optics express, 2022, 30(12)：21854-21865.

[6] BELKIN M, CHAO S H, JONSSON M P, et al. Plasmonic nanopores for trapping, controlling displacement, and sequencing of DNA[J]. ACS nano, 2015, 9(11): 10598-10611.

[7] NICOLI F, VERSCHUEREN D, KLEIN M, et al. DNA translocations through solid-state plasmonic nanopores[J]. Nano letters, 2014, 14(12): 6917-6925.

[8] FARAMARZI V, AHMADI V, FOTOUHI B, et al. A potential sensing mechanism for DNA nucleobases by optical properties of GO and MoS_2 nanopores[J]. Scientific reports, 2019, 9: 1-11.

[9] ABASIFARD M, AHMADI V, FOTOUHI B, et al. DNA nucleobases sensing by localized plasmon resonances in graphene quantum dots with nanopore: a first principle approach[J]. The journal of physical chemistry C, 2019, 123(41): 25309-25319.

[10] FOOUHI B, AHMADI V, ABASIFARD M, et al. Interband π plasmon of graphene nanopores: a potential sensing mechanism for DNA nucleotides[J]. Journal of physical chemistry C, 2016, 120: 13693-13700.

[11] FOTOUHI B, AHMADI V, ABASIFARD M. Controlling DNA translocation speed through graphene nanopore via plasmonic fields[J]. Scientia iranica, 2018, 25(3): 1849-1856.

[12] WANG Y, CHENG M, WANG L, et al. Nanocrystalline graphite nanopores for DNA sensing[J]. Carbon, 2021, 176: 271-278.

[13] DRAINE B T, FLATAU P J. Discrete-dipole approximation for scattering calculations[J]. Journal of Optical Society of America A, 1994, 11: 1491-1499.

[14] WALTER M, HAKKINEN H, LEHTOVAARA L, et al. Time-dependent density-functional theory in the projector augmented-wave method[J]. The journal of chemical physics, 2008, 128(24): 244101.

[15] SAKKO A, ROSSI T P, NEIMINEN R M. Dynamical coupling of plasmons and molecular excitations by hybrid quantum/classical calculations: time-domain approach[J]. Journal of physics: condensed matter, 2014, 26(31): 315013.

[16] MORTENSEN J J, HANSEN L B, JACOBSEN K W. Real-space grid implementation of the projector augmented wave method[J]. Physical review B, 2005, 71(3): 035109.

[17] AMENDOLA V, BAKR O M, STELLACCI F. A study of the surface plasmon resonance of silver nanoparticles by the discrete dipole approximation method: effect of shape, size, structure, and assembly[J]. Plasmonics, 2010, 5: 85-97.

[18] PERASSI E M, HRELESCU C, WINSNET A, et al. Quantitative understanding of the optical properties of a single, complex-shaped gold nanoparticle from experiment and theory[J]. ACS nano, 2014, 8(5): 4395-4402.

[19] GAO Y, NEUHAUSER D. Dynamical quantum-electrodynamics embedding : combining time-dependent density functional theory and the near-field method[J]. The journal of chemical physics, 2012, 137(7): 074113.

[20] COOMAR A, ARNTSEN C, LOPATA K A, et al. Near-field: a finite-difference time-dependent method for simulation of electrodynamics on small scales[J]. The journal of chemical physics, 2011, 135(8): 084121.

[21] NELSON F J, KAMINENI V K, ZHANG T, et al. Optical properties of large-area polycrystalline chemical vapor deposited graphene by spectroscopic ellipsometry[J]. Applied physics letters, 2010, 97(25): 253110.

[22] GRAY A, BALOOCH M, ALLEGRET S, et al. Optical detection and characterization of graphene by broadband spectrophotometry[J]. Journal of applied physics, 2008, 104(5): 053109.

[23] WANG W E, BALLOCH M, CLAYPOOL C, et al. Combined reflectometry-ellipsometry technique to measure graphite down to monolayer thickness[J]. Solid state technology, 2009, 52(6): 18-22.

[24] WEBER J W, CALADO V E, VAN DE SANDEN M C M. Optical constants of graphene measured by spectroscopic ellipsometry[J]. Applied physics letters, 2010, 97(9): 091904.

[25] ENKOVAARA J, ROMERO N A, SHENDE S, et al. GPAW-massively parallel electronic structure calculations with Python-based software[J]. Procedia computer science, 2011, 4: 17-25.

[26] BAHN S R, JACOBSEN K W. An object-oriented scripting interface to a legacy electronic structure code[J]. Computing in science & engineering, 2000, 4(3): 56-66.

[27] ZHOU W, LEE J, NANDA J, et al. Atomically localized plasmon enhancement in monolayer graphene[J]. Nature nanotechnology, 2012, 7(3): 161-165.

[28] DESPOJA V, NOVKO D, DEKANIC K, et al. Two-dimensional and π plasmon spectra in pristine and doped graphene[J]. Physical review B, 2013, 87(7): 075447.

[29] HU J, ZENG H, WANG C, et al. Interband π plasmon of graphene: strong small-size and field-enhancement effects[J]. Physical chemistry chemical physics, 2014, 16(42): 23483-23491.